Measurement of α_s in Hadronic Z Decays Using All-Orders Resummed Predictions

The ALEPH Collaboration[1]

Abstract

Using 109000 hadronic events obtained with the ALEPH detector at LEP at energies close to the Z resonance peak, the strong coupling constant $\alpha_s(M_Z^2)$ is determined from an analysis of the global event shape variables thrust, heavy jet mass and the differential two-jet rate based on the k_T-clustering scheme. The analysis uses improved theoretical predictions in which leading and next-to-leading logarithms, resummed to all orders, supplement second order expressions. After combining the results from all variables, $\alpha_s(M_Z^2)$ is measured to be 0.125 ± 0.005, where the error is the quadratic sum of experimental and theoretical uncertainties, and is dominated by the latter.

(Submitted to Physics Letters B)

---

[1] See the following pages for the list of authors.

The ALEPH Collaboration

D. Decamp, B. Deschizeaux, C. Goy, J.-P. Lees, M.-N. Minard

Laboratoire de Physique des Particules (LAPP), IN[2]P[3]-CNRS, 74019 Annecy-le-Vieux Cedex, France

R. Alemany, F. Ariztizabal, P. Comas, J.M. Crespo, M. Delfino, E. Fernandez, V. Gaitan, Ll. Garrido, Ll.M. Mir, A. Pacheco, A. Pascual

Institut de Fisica d'Altes Energies, Universitat Autonoma de Barcelona, 08193 Bellaterra (Barcelona), Spain[8]

D. Creanza, M. de Palma, A. Farilla, G. Iaselli, G. Maggi, M. Maggi, S. Natali, S. Nuzzo, M. Quattromini, A. Ranieri, G. Raso, F. Romano, F. Ruggieri, G. Selvaggi, L. Silvestris, P. Tempesta, G. Zito

INFN Sezione di Bari e Dipartimento di Fisica dell' Università, 70126 Bari, Italy

Y. Gao, H. Hu,[21] D. Huang, X. Huang, J. Lin, J. Lou, C. Qiao,[21] T. Wang, Y. Xie, D. Xu, R. Xu, J. Zhang, W. Zhao

Institute of High-Energy Physics, Academia Sinica, Beijing, The People's Republic of China[9]

W.B. Atwood,[2] L.A.T. Bauerdick, E. Blucher, G. Bonvicini, F. Bossi, J. Boudreau, T.H. Burnett,[3] H. Drevermann, R.W. Forty, R. Hagelberg, S. Haywood, J. Hilgart, R. Jacobsen, B. Jost, M. Kasemann,[26] J. Knobloch, E. Lançon, I. Lehraus, T. Lohse, A. Lusiani, M. Martinez, P. Mato, T. Mattison, H. Meinhard, S. Menary,[27] T. Meyer, A. Minten, A. Miotto, R. Miquel, H.-G. Moser, J. Nash, P. Palazzi, J.A. Perlas, F. Ranjard, G. Redlinger, L. Rolandi,[28] A. Roth,[30] J. Rothberg,[3] T. Ruan,[21,33] M. Saich, D. Schlatter, M. Schmelling, F. Sefkow, W. Tejessy, H. Wachsmuth, W. Wiedenmann, T. Wildish, W. Witzeling, J. Wotschack

European Laboratory for Particle Physics (CERN), 1211 Geneva 23, Switzerland

Z. Ajaltouni, F. Badaud, M. Bardadin-Otwinowska, A.M. Bencheikh, R. El Fellous, A. Falvard, P. Gay, C. Guicheney, P. Henrard, J. Jousset, B. Michel, J-C. Montret, D. Pallin, P. Perret, B. Pietrzyk, J. Proriol, F. Prulhière, G. Stimpfl

Laboratoire de Physique Corpusculaire, Université Blaise Pascal, IN[2]P[3]-CNRS, Clermont-Ferrand, 63177 Aubière, France

J.D. Hansen, J.R. Hansen, P.H. Hansen, R. Møllerud, B.S. Nilsson

Niels Bohr Institute, 2100 Copenhagen, Denmark[10]

I. Efthymiopoulos, A. Kyriakis, E. Simopoulou, A. Vayaki,[1] K. Zachariadou

Nuclear Research Center Demokritos (NRCD), Athens, Greece

J. Badier, A. Blondel, G. Bonneaud, J.C. Brient, G. Fouque, A. Gamess, J. Harvey, S. Orteu, A. Rosowsky, A. Rougé, M. Rumpf, R. Tanaka, H. Videau

Laboratoire de Physique Nucléaire et des Hautes Energies, Ecole Polytechnique, IN[2]P[3]-CNRS, 91128 Palaiseau Cedex, France

D.J. Candlin, M.I. Parsons, E. Veitch

Department of Physics, University of Edinburgh, Edinburgh EH9 3JZ, United Kingdom[11]

L. Moneta, G. Parrini

Dipartimento di Fisica, Università di Firenze, INFN Sezione di Firenze, 50125 Firenze, Italy

M. Corden, C. Georgiopoulos, M. Ikeda, J. Lannutti, D. Levinthal,[16] M. Mermikides[†], L. Sawyer, S. Wasserbaech

Supercomputer Computations Research Institute and Dept. of Physics, Florida State University, Tallahassee, FL 32306, USA [13,14,15]

A. Antonelli, R. Baldini, G. Bencivenni, G. Bologna,[5] P. Campana, G. Capon, F. Cerutti, V. Chiarella, B. D'Ettorre-Piazzoli,[32] G. Felici, P. Laurelli, G. Mannocchi,[6] F. Murtas, G.P. Murtas, L. Passalacqua, M. Pepe-Altarelli, P. Picchi[5]

Laboratori Nazionali dell'INFN (LNF-INFN), 00044 Frascati, Italy

B. Altoon, O. Boyle, P. Colrain, I. ten Have, J.G. Lynch, W. Maitland, W.T. Morton, C. Raine, J.M. Scarr, K. Smith, A.S. Thompson, R.M. Turnbull

Department of Physics and Astronomy, University of Glasgow, Glasgow G12 8QQ, United Kingdom[11]

B. Brandl, O. Braun, R. Geiges, C. Geweniger, P. Hanke, V. Hepp, E.E. Kluge, Y. Maumary, A. Putzer, B. Rensch, A. Stahl, K. Tittel, M. Wunsch

Institut für Hochenergiephysik, Universität Heidelberg, 6900 Heidelberg, Fed. Rep. of Germany[17]

A.T. Belk, R. Beuselinck, D.M. Binnie, W. Cameron, M. Cattaneo, D.J. Colling, P.J. Dornan,[1] S. Dugeay, A.M. Greene, J.F. Hassard, N.M. Lieske, S.J. Patton, D.G. Payne, M.J. Phillips, J.K. Sedgbeer, G. Taylor, I.R. Tomalin, A.G. Wright

Department of Physics, Imperial College, London SW7 2BZ, United Kingdom[11]

P. Girtler, D. Kuhn, G. Rudolph

Institut für Experimentalphysik, Universität Innsbruck, 6020 Innsbruck, Austria[19]

C.K. Bowdery, T.J. Brodbeck, A.J. Finch, F. Foster, G. Hughes, D. Jackson, N.R. Keemer, M. Nuttall, A. Patel, T. Sloan, S.W. Snow, E.P. Whelan

Department of Physics, University of Lancaster, Lancaster LA1 4YB, United Kingdom[11]

T. Barczewski, K. Kleinknecht, J. Raab, B. Renk, S. Roehn, H.-G. Sander, H. Schmidt, F. Steeg, S.M. Walther, B. Wolf

Institut für Physik, Universität Mainz, 6500 Mainz, Fed. Rep. of Germany[17]

J-J. Aubert, C. Benchouk, V. Bernard, A. Bonissent, J. Carr, P. Coyle, J. Drinkard, F. Etienne, S. Papalexiou, P. Payre, Z. Qian, D. Rousseau, P. Schwemling, M. Talby

Centre de Physique des Particules, Faculté des Sciences de Luminy, IN²P³-CNRS, 13288 Marseille, France

S. Adlung, H. Becker, W. Blum,[1] D. Brown, P. Cattaneo,[29] G. Cowan, B. Dehning, H. Dietl, F. Dydak,[25] M. Fernandez-Bosman, M. Frank, A.W. Halley, T. Hansl-Kozanecka,[2,22] J. Lauber, G. Lütjens, G. Lutz, W. Männer, Y. Pan, R. Richter, H. Rotscheidt, J. Schröder, A.S. Schwarz, R. Settles, U. Stierlin, U. Stiegler, R. St. Denis, M. Takashima,[4] J. Thomas,[4] G. Wolf

Max-Planck-Institut für Physik und Astrophysik, Werner-Heisenberg-Institut für Physik, 8000 München, Fed. Rep. of Germany[17]

V. Bertin, J. Boucrot, O. Callot, X. Chen, A. Cordier, M. Davier, J.-F. Grivaz, Ph. Heusse, P. Janot, D.W. Kim,[20] F. Le Diberder, J. Lefrançois,[1] A.-M. Lutz, M.-H. Schune, J.-J. Veillet, I. Videau, Z. Zhang, F. Zomer

Laboratoire de l'Accélérateur Linéaire, Université de Paris-Sud, IN²P³-CNRS, 91405 Orsay Cedex, France

D. Abbaneo, S.R. Amendolia, G. Bagliesi, G. Batignani, L. Bosisio, U. Bottigli, C. Bradaschia, M. Carpinelli, M.A. Ciocci, R. Dell'Orso, I. Ferrante, F. Fidecaro,[1] L. Foà, E. Focardi, F. Forti, C. Gatto, A. Giassi, M.A. Giorgi, F. Ligabue, E.B. Mannelli, P.S. Marrocchesi, A. Messineo, F. Palla, G. Rizzo, G. Sanguinetti, J. Steinberger, R. Tenchini, G. Tonelli, G. Triggiani, C. Vannini, A. Venturi, P.G. Verdini, J. Walsh

Dipartimento di Fisica dell'Università, INFN Sezione di Pisa, e Scuola Normale Superiore, 56010 Pisa, Italy

J.M. Carter, M.G. Green, P.V. March, T. Medcalf, I.S. Quazi, J.A. Strong, L.R. West

Department of Physics, Royal Holloway & Bedford New College, University of London, Surrey TW20 OEX, United Kingdom[11]

D.R. Botterill, R.W. Clifft, T.R. Edgecock, M. Edwards, S.M. Fisher, T.J. Jones, P.R. Norton, D.P. Salmon, J.C. Thompson

Particle Physics Dept., Rutherford Appleton Laboratory, Chilton, Didcot, Oxon OX11 OQX, United Kingdom[11]

3

B. Bloch-Devaux, P. Colas, W. Kozanecki,[2] M.C. Lemaire, E. Locci, S. Loucatos, E. Monnier, P. Perez, F. Perrier, J. Rander, J.-F. Renardy, A. Roussarie, J.-P. Schuller, J. Schwindling, D. Si Mohand, B. Vallage

Service de Physique des Particules, DAPNIA, CE-Saclay, 91191 Gif-sur-Yvette Cedex, France[18]

R.P. Johnson, A.M. Litke, J. Wear

Institute for Particle Physics, University of California at Santa Cruz, Santa Cruz, CA 95064, USA

J.G. Ashman, W. Babbage, C.N. Booth, C. Buttar, R.E. Carney, S. Cartwright, F. Combley, F. Hatfield, J. Martin, D. Parker, P. Reeves, L.F. Thompson

Department of Physics, University of Sheffield, Sheffield S3 7RH, United Kingdom[11]

E. Barberio, S. Brandt, C. Grupen, L. Mirabito,[31] U. Schäfer, H. Seywerd

Fachbereich Physik, Universität Siegen, 5900 Siegen, Fed. Rep. of Germany[17]

G. Ganis,[35] G. Giannini, B. Gobbo, F. Ragusa[24]

Dipartimento di Fisica, Università di Trieste e INFN Sezione di Trieste, 34127 Trieste, Italy

L. Bellantoni, D. Cinabro,[34] J.S. Conway, D.F. Cowen,[23] Z. Feng, D.P.S. Ferguson, Y.S. Gao, J. Grahl, J.L. Harton, R.C. Jared,[7] B.W. LeClaire, C. Lishka, Y.B. Pan, J.R. Pater, Y. Saadi, V. Sharma, M. Schmitt, Z.H. Shi, Y.H. Tang, A.M. Walsh, F.V. Weber, M.H. Whitney, Sau Lan Wu, X. Wu, G. Zobernig

Department of Physics, University of Wisconsin, Madison, WI 53706, USA[12]

1 Introduction

The strong coupling constant α_s is the only free parameter of Quantum Chromodynamics (QCD). In the framework of the standard model of strong and electroweak interactions, it is related to one out of three fundamental gauge couplings, and it is the coupling constant which is least well known.

The best measurements of α_s in Z decays have resulted from the analysis of hadronic final states by comparing jet rates [1–7], distributions of global event shape variables [1, 8, 6, 7] and energy-energy correlations [8, 9, 10, 11, 6] with second order QCD predictions (e.g. [12, 13]). The systematic precision has been limited by the necessity to compare a hadronic final state with a second order partonic state (with at most four partons), and by the residual dependence of the theoretical predictions on the choice of the renormalization scale, μ [13].

Although QCD predictions to $\mathcal{O}(\alpha_s^3)$ are not within immediate reach, there has recently been significant theoretical progress concerning the resummation of large logarithms in the perturbation series to all orders of α_s, performed by S. Catani et al. [14, 15, 16]. This reduces the uncertainties related to the transition between the perturbatively computable parton level and the hadron level as well as the uncertainties related to the renormalization scale. It also extends the range of validity of the predictions into the region where the emitted gluons are close in phase-space to the original quarks (the so-called two-jet region), and where the experimental statistics are high. In particular, all leading and next-to-leading logarithms have been resummed for the global event shape variables thrust [14], and heavy jet mass [15]. Also the logarithms in the expressions for jet multiplicities are known to exponentiate in the case that jets are defined by a proper clustering scheme (defined in section 2). For these multiplicities all leading logarithms and part of the next-to-leading logarithms have been resummed [16].

In this paper, the variables thrust, T, heavy jet mass with respect to the thrust axis, $\rho = M_h^2/s$, and differential two-jet rate, y_3, are (re-)analyzed in the framework of the additional theoretical results. After a brief recapitulation of the event selection and data analysis in section 2, section 3 summarizes the theoretical predictions. The uncertainties due to the hadronization process and unknown higher orders are discussed in sections 4 and 5. The final measurement for α_s is presented in section 6; section 7 contains the conclusions.

2 Event Selection and Data Analysis

The ALEPH detector, which provides both tracking information and calorimetry over almost the full solid angle, is described elsewhere [17]. The analysis is based on 109000 hadronic events at center-of-mass energies in the range 91.0 GeV $\leq \sqrt{s} \leq$ 91.5 GeV. Only charged particles measured in the tracking chambers of the ALEPH detector are used and the pion mass is assigned to them. The event and track selection is identical to that used previously [1, 8].

The experimental distributions are corrected using hadronic event generators and the ALEPH detector simulation program for the effects of geometrical acceptance, detector efficiency and resolution, decays, neutral particles, secondary interactions, and initial state photon radiation. All distributions are in addition corrected back to a fixed center of mass energy, $\sqrt{s} = 91.2$ GeV. The corrections are dominated by the cuts defining the geometrical acceptance. In order to keep the corrections for neutral particles small, the total visible energy of charged particles is used in the computation of all event shape variables instead of the center of mass energy. The inclusion of the calorimetric information on neutral particles would result in a loss of experimental resolution, especially in the two-jet region. The systematic experimental errors are estimated by varying selection cuts and by employing different event generators tuned to describe the overall structure

of hadronic final states [18].

The analysis is based on the distributions of the global event shape variables thrust (T), heavy jet mass with respect to the thrust axis (ρ) and the differential two-jet rate (y_3). Definitions can be found in reference [13]. The variable y_3 is used in the context of the k_T-clustering algorithm [16, 19]. For this algorithm each final state particle is initially considered as a jet. For each pair i,j of jets the metric

$$y_{ij} = \frac{2\min\left(E_i^2, E_j^2\right)}{E_{vis}^2}\left(1 - \cos\Theta_{i,j}\right) \equiv \frac{4k_T^2}{E_{vis}^2} \tag{1}$$

is evaluated, where Θ_{ij} is the opening angle between the three-momentum vectors of the jets and k_T is the smallest of the two transverse momenta of the jets with respect to the axis dividing Θ_{ij} into two equal angles. The pair with smallest y_{ij} is merged into a single jet by adding the corresponding four-momenta ("E-scheme" recombination). The procedure is iterated until exactly three jets are left, at which point the smallest y_{ij} defines y_3.

3 Theoretical Predictions

Previous ALEPH measurements [1, 8] of $\alpha_s(M_Z^2)$ using event shape variables were based on exact second order matrix-elements [12], which were integrated to predict distributions for suitable event-shape variables following the procedure of [13]. For any event shape variable X, the second order predictions for the cumulative distribution, defined by

$$R(y, \alpha_s) = \frac{1}{\sigma_{tot}}\sigma(X < y) \quad, \tag{2}$$

can be expressed as

$$\ln R(y, \alpha_s) = \alpha_s A(y) + \alpha_s^2 B(y) + \mathcal{O}(\alpha_s^3) \quad. \tag{3}$$

Here and in the following the explicit dependence on the renormalization scale, μ, is dropped in the arguments for simplicity. The functions A and B are specific for the event shape variable and are obtained from appropriate integrals over the first and second order matrix elements.

Alternative expansions of $\ln R$ in terms of the logarithms $L \equiv -\ln y$, as displayed in table 1, have been performed in the case of $y = 1 - T, \rho, y_3$. These logarithms become large in the two-jet region. The expansion can be expressed in the form

$$\ln R(y, \alpha_s) = L \cdot f_{LL}(\alpha_s L) + f_{NLL}(\alpha_s L) + \mathcal{O}\left(\frac{1}{L}\cdot(\alpha_s L)^n\right) \quad. \tag{4}$$

The functions f_{LL} and f_{NLL} depend only on the product of α_s and L. The first two terms in eq. (4) represent the leading and the next-to-leading logarithms. They have been computed for the variables $1-T$, ρ and (partially) for y_3 in [14, 15, 16]. The following terms are called subleading and have not been calculated in [14, 15, 16].

The relationship between eq. (3) and eq. (4) becomes apparent when the latter is in addition expanded in powers of α_s:

$$\ln R(y, \alpha_s) = \sum_{n=1}^{\infty} \alpha_s^n\left(a_n L^{n+1} + b_n L^n + \cdots\right) \quad. \tag{5}$$

This expansion is shown schematically in table 1. The first column ($\propto \alpha_s^n L^{n+1}$) represents the leading logarithms, the second column ($\propto \alpha_s^n L^n$) the next-to-leading logarithms and the first two rows represent the complete $\mathcal{O}(\alpha_s^2)$ predictions of eq. (3).

An improved prediction thus can be constructed by combining the exact second order predictions of eq. (3) with the leading and next-to-leading logarithms of eq. (4), starting in $\mathcal{O}(\alpha_s^3)$. There are several ways this matching can be done.

- The contributions up to $\mathcal{O}(\alpha_s^2)$ can be subtracted from the resummed expression of $\ln R$ in eq. (4) and the result added to the complete second order prediction in eq. (3). From this the prediction for R is derived by taking the exponential, and finally the distribution dR/dL is determined by differentiation. This method will in the following be called "$\ln R$ matching".

- In analogy, the second order prediction for R, instead of $\ln R$, can be combined with the exponential of the all-order resummed leading and next-to-leading expression for $\ln R$. This will be called "R matching".

- An intermediate matching method can be used as well[2], where all the known logarithmic terms (including the known subleading term proportional to $\alpha_s^2 L$) are exponentiated.

All these matching schemes lead to predictions which contain the complete $\mathcal{O}(\alpha_s^2)$ part and all resummed logarithms. The differences, which are due to different schemes for the exponentiation of the corrections, are of $\mathcal{O}(\alpha_s^3)$; they are subleading for thrust and heavy jet mass and next-to-leading in the case of y_3, since not all next-to-leading terms have been computed for y_3. The third scheme is in principle best justified theoretically when a complete calculation is considered. This is not necessarily true, however, when the perturbation series is truncated at the next-to-leading order. All three schemes are therefore considered as realistic approaches in this analysis. Since the $\ln R$ and the intermediate matching are found to produce results which are practically identical, only the differences between the $\ln R$ and the R matching schemes will be used to assess one of the theoretical uncertainties, which is referred to as the matching ambiguity.

In view of the improvement of the theoretical predictions obtained when using the new calculations [14, 15, 16], the role of the renormalization scale parameter, μ, has to be rediscussed. The explicit μ-dependencies of the different terms in eq. (3) are given in [13]. Those for eq. (4) can be found in [14],[15] for $1 - T$ and ρ, and in the appendix for y_3. In the past, when comparing data with second order calculations, very small values of the renormalization scale have been used with the goal of mimicking the large missing higher than second order corrections [2, 4, 6]. The introduction of such small scales results in the addition of some terms of the next-to-leading logarithmic type to the prediction.

Since leading and next-to-leading terms are now included to all orders in the theoretical prediction, there is no longer motivation to consider small scales [14, 20]. These would introduce large terms $\ln \mu^2/Q^2$ in all orders in the perturbation series which are not any longer needed to compensate unknown leading and next-to-leading logarithms. Therefore, the convergence of the perturbation series would deteriorate. Nevertheless, moderate changes of the scale around the so-called natural value, $f \equiv \mu^2/s = 1$, will be allowed for as estimates of theoretical uncertainties.

The fits to the experimental distributions have been performed with two independent implementations of the theoretical predictions. In one case the functions A and B in eq. (3) have been computed for the variables $- \ln y_3$, $- \ln(1 - T)$ and $- \ln \rho$, using the appropriately modified integration program EVENT [21]. The resulting second order predictions were then combined with the formulae in [14, 15, 16] in the way indicated above. Independently, the original program [22] of the authors of references [14, 15, 16] including the combination with the second order calculation was used. The differences between the two implementations were found to be negligible.

---

[2]This scheme is defined by equations (3) and (4) in reference [14].

4 Correction for Hadronization

The theoretical predictions described above concern a purely partonic final state and do not deal with the hadronization of these partons. The predictions therefore have to be folded by a response matrix [1] which has to be determined using fragmentation models. They have to be chosen such that the hadronization starts from partonic final states corresponding as closely as possible to the analytic perturbative calculations.

Most suited are therefore parton shower (PS) models based on the probabilistic interpretation of the leading-log approximation [23, 24]. In this analysis, the Lund PS model [25] (version 7.2) as implemented in the JETSET package and the HERWIG [24] generator (version 5.3) are used. The models have been tuned [18] and describe well the general structure of the hadronic final state. There are important differences between the Lund PS model and HERWIG:

- The hadronization in Lund PS is based on the break-up of color strings [26] between final state partons, while HERWIG uses a cluster fragmentation scheme [27].

- The first branching in the parton shower follows the exact $\mathcal{O}(\alpha_s)$ matrix element in Lund PS while HERWIG uses the leading-log approximation already in first order.

- Effects of gluon coherence [28] and spin correlations [29] (which are partly beyond leading logarithmic order) are taken into account to a larger extent in HERWIG than in Lund PS.

The differences between the corrections as derived from Lund PS and HERWIG are therefore included as part of the hadronization uncertainties.

Although PS models resemble closely the structure of the analytic formulae, the correspondence is not perfect:

- Parton showers have to be stopped after a finite number of branchings when the virtual masses of the partons have reached a non-perturbative regime of $Q_0 \approx 1\mathrm{GeV}$. The exponentiation of leading logarithms, however, corresponds to a sum over all branchings down to a Q_0 of the order of the QCD scale, Λ.

- PS models contain leading logarithms but not all of the next-to-leading logarithms. Since the models are tuned to describe the data, missing terms can be effectively accounted for by the hadronization process. Some of the next-to-leading logarithms may therefore be double-counted due to the folding of the hadronization correction.

- PS models do not contain the full $\mathcal{O}(\alpha_s^2)$ while it is present in the theoretical predictions. The subleading terms of second order may therefore be double-counted. In the case of HERWIG the same is true even for the $\mathcal{O}(\alpha_s)$.

The corresponding uncertainties are estimated in the following way:

- The parton showers are stopped at different values Q_0 of virtual parton masses. For each value the corrections for hadronization are computed. The dependence on Q_0 is then used to extrapolate the correction (linearly) from $Q_0 \approx 1\mathrm{GeV}$ to $Q_0 = 0$. These extrapolations are found to be very small. They correspond to changes in the fit value for $\alpha_s(M_Z^2)$ around 0.001 in all cases.

- The differences between Lund PS and HERWIG contain a combination of hadronization uncertainties and double-counting effects. In order to isolate the double-counting, Lund PS is also used with the explicit $\mathcal{O}(\alpha_s)$ matrix elements switched off. The influence of the missing $\mathcal{O}(\alpha_s)$ should result in a realistic estimate of the systematic effects since all possible double counting for Lund PS is of higher order.

8

The error due to hadronization corrections is defined as the quadratic sum of the full size of the change in α_s due to the extrapolation of the corrections to $Q_0 = 0$ and half the range of corrected values of α_s obtained by using the three PS models HERWIG, Lund PS, and Lund PS without the $\mathcal{O}(\alpha_s)$ matrix element. The corrected value of α_s is taken to be the center of this range, extrapolated to $Q_0 = 0$.

The fit ranges were chosen such that the hadronization corrections for the theoretical predictions stay below 10%. In addition it was required that the fit ranges do not approach the three parton phase-space boundary (2/3 for thrust, 1/3 for heavy jet mass and 1/3 for the differential two-jet rate), where the resummed logarithms are no longer large and therefore the matching ambiguities due to the omission of sub-leading terms start to be big. The fit ranges which meet these criteria are $[1.6, 4.0]$ for the variable $-\ln y_3$, $[1.2, 2.6]$ for $-\ln(1-T)$, and $[1.8, 2.8]$ for $-\ln \rho$. These fit ranges are considerably larger than the ones used in the earlier ALEPH analysis [1] even though the requirement for the maximal size of the hadronization corrections was weaker.

An example is given in table 2, where the fit values of $\alpha_s(M_Z^2)$ (using the R matching and scale parameter $f = 1$), extrapolated to $Q_0 = 0$, are shown for the uncorrected case, after correction by the three PS models, and for the center of the range spanned by the models. It can be seen that the fit results change only slightly when leaving out the exact $\mathcal{O}(\alpha_s)$ matrix element in the Lund PS model, in contrast to the naive expectation of an $\mathcal{O}(\alpha_s)$ (i.e. $\approx 10\%$) difference. This is explained by the fact that the main differences between the two tuned models occur for the parameters governing the perturbative parton shower, while those governing the hadronization process are almost identical [18].

5   Theoretical Uncertainties

Two methods have been used to estimate the theoretical uncertainties in the QCD prediction:

- Applying the $\ln R$ and R matching schemes as described in section 3.
- Changing the renormalization scale in a limited range of $-1 \leq \ln f \leq +1$ around its natural value $\ln f = 0$. These scale variations are somewhat larger than those used in [14].

The central value of α_s is taken as the mean of the results using the two matching schemes at $\ln f = 0$. The theoretical error is defined to be the maximum difference between this central value and the fit results obtained from all combinations of scales and matching schemes. The theoretical uncertainties are found to be small for the differential two-jet rate (± 0.0043) and slightly larger for thrust (± 0.0065) and the heavy jet mass (± 0.0057).

Fig. 1 exhibits the dependence of α_s on the renormalization scale parameter f. The bands represent the ranges covered by the different matching schemes. For illustration, these dependences are also shown in the case that pure first order predictions or pure second order predictions are used without applying any further correction for missing higher orders. In these cases the R and $\ln R$ matching schemes are defined in analogy to the case of the full prediction,

$$\ln R \text{ matching:} \quad R(y) = \exp\left(\alpha_s A(y) \left[+\alpha_s^2 B(y)\right]\right)$$
$$R \text{ matching:} \quad R(y) = 1 + \alpha_s A(y) \left[+\alpha_s^2 \left(B(y) + \frac{1}{2} A^2(y)\right)\right] \quad , \qquad (6)$$

where the terms within squared brackets only apply to the second order case. It is seen from fig. 1 that both, scale dependencies and matching dependencies, drop drastically from first order to second order and finally to second order improved by resummed logarithms. This reflects the expected improvement in the rate of convergence of the perturbative series after the inclusion of the resummed terms.

9

In the case of thrust and heavy jet mass, the scale dependence is the dominant uncertainty while the matching ambiguity dominates the theoretical error for y_3. This larger matching ambiguity for y_3 may be due to the next-to-leading terms missing in [16].

The scale dependence for y_3 vanishes locally around the natural scale. On the other hand, for $\ln f$ below -1.5, the scale dependence becomes very strong. At the same time, the quality of the fit degrades, as can be seen in fig. 2. Similar but somewhat weaker trends are observed for the other two variables, also shown in fig. 2.

A number of checks have been performed to ensure that the theoretical errors are not underestimated. They include:

- Dropping the second order terms not included in the resummation of large logarithms and repeating the fit. The maximum variation in the fitted value of α_s is well within the theoretical errors.

- Adding or subtracting an estimate of the unknown third order terms obtained from the corresponding second order terms, rescaled by the ratio of the second and first orders. The maximum change is again within the theoretical errors.

- Moving the phase space boundary. In the implementation of the theoretical predictions used in the fits all unknown subleading terms are replaced by a constant such that $\ln R = 0$ at the phase space boundary for the event shape variable under consideration. This ensures that the differential distribution is properly normalized to the total cross-section. One can argue that, since the predictions are complete only to $\mathcal{O}(\alpha_s^2)$, the normalization should be performed at the phase space boundary for a four-parton final state [22]. The effects of this modification, as well as the effects of removing altogether the constraint, have been found to be negligible.

For comparison, an exponentiation of part of the leading infrared corrections, as suggested in [30], has been combined with the second order prediction[3]. The results agree with the approach described above within the 5% accuracy claimed in [30], except for the case of the heavy jet mass, for which the discrepancy is almost 9%.

6 Fit Results

As can be seen from fig. 3, the theoretical predictions are in good agreement with the data inside the previously defined fit ranges for all three variables $-\ln y_3$, $-\ln(1-T)$, $-\ln\rho$. Even in the two-jet region outside the fit ranges, where hadronization corrections as well as corrections due to detector effects are very large, reasonable agreement is found. The tail towards the three parton phase space limit is also well reproduced by the predictions for the variables $-\ln y_3$ and $-\ln(1-T)$. This tail is less well described for the $-\ln\rho$ distribution. In this case the fit quality becomes poor if the fit range in fig. 3 is extended by one or two data points towards the left. The resulting values for $\alpha_s(M_Z^2)$, however, do not change significantly compared to the systematic errors. The other two variables turn out to be insensitive to any small variations in the fit ranges.

---

[3]The simple procedure used in [30] to obtain the improved α_s values amounts essentially to a constant shift of around 10% with respect to the results obtained with pure second order predictions. On the contrary, in this comparison the matrix elements are explicitly modified following the exponentiation prescription of [30] before applying hadronization corrections. The resulting fits lead to different shifts for the α_s values obtained from the three variables.

Using the above definitions of hadronization uncertainties and uncertainties in the theoretical predictions, the results from the three distributions are found to be

$$
\begin{aligned}
\alpha_s(M_Z^2)|_{y_3} &= 0.1257 \pm 0.0010_{stat} \pm 0.0025_{syst} \pm 0.0007_{hadr} \pm 0.0043_{theo} \\
\alpha_s(M_Z^2)|_T &= 0.1263 \pm 0.0008_{stat} \pm 0.0010_{syst} \pm 0.0028_{hadr} \pm 0.0065_{theo} \qquad (7) \\
\alpha_s(M_Z^2)|_\rho &= 0.1243 \pm 0.0010_{stat} \pm 0.0033_{syst} \pm 0.0042_{hadr} \pm 0.0057_{theo} \quad ,
\end{aligned}
$$

where the first error is statistical, the second estimates the experimental systematics, the third concerns the hadronization correction, and the last is the estimate of theoretical uncertainties.

In order to derive a combined value for α_s, weighted averages of all the individual fit results that were used in the definition of the errors are computed. In each case the statistical errors of the values of α_s obtained for the three variables are conservatively assumed to be fully correlated. The analysis is then redone in the same way as for individual event shape variables. The weights in the average are chosen to optimally exploit the independent information in the three measurements for α_s which is reflected in the final overall error reaching a minimum. The combined measurement which thus takes into account the correlations between all systematic errors is given by

$$
\alpha_s(M_Z^2) = 0.1251 \pm 0.0009_{stat} \pm 0.0021_{syst} \pm 0.0007_{hadr} \pm 0.0038_{theo} \quad . \qquad (8)
$$

If the weights are simply taken to be the inverse of the squared overall errors of the individual measurements, the final result does not noticeably change. After adding all errors in quadrature, the combined measurement corresponds to $\alpha_s(M_Z^2) = 0.125 \pm 0.005$. This number is compatible with the earlier ALEPH measurements [1, 8] but carries a significantly smaller error.

7 Conclusions

A new measurement of $\alpha_s(M_Z^2)$ has been performed using the global event shape variables thrust, heavy jet mass and differential two-jet rate, and exploiting improved theoretical predictions which combine second order matrix elements with an all-order resummation of leading and next-to-leading logarithms. These lead to a better description of the data without the necessity to introduce small renormalization scales. The combined result of the measurements, $\alpha_s = 0.125 \pm 0.005$, agrees with the earlier ALEPH measurements but is more precise by almost a factor two. The overall uncertainty is still dominated by theoretical errors.

Acknowledgements

Appendix: Prediction for y_3 Including Scale Dependence

The resummed expression (before combining it with the second order prediction) for $\ln R(y_3)$ is given in [16] as

$$\ln R(y_3) = -2\frac{C_F}{\pi} \int_{\sqrt{sy_3}}^{\sqrt{s}} \frac{dq}{q} \alpha_s(q^2) \left(\ln \frac{s}{q^2} - \frac{3}{2} \right) \quad , \tag{9}$$

with $C_F = 4/3$. The explicit dependence on the renormalization scale μ is obtained by expanding $\alpha_s(q^2)$ in terms of $\alpha_s(\mu^2)$, using the solution

$$\alpha_s(q^2) = \frac{\alpha_s(\mu^2)}{w} \left(1 - \frac{b_1}{b_0} \frac{\alpha_s(\mu^2)}{w} \ln w \right) \tag{10}$$

of the renormalization group equation

$$\mu^2 \frac{d\alpha_s}{d\mu^2} = -b_0 \alpha_s^2 - b_1 \alpha_s^3 + \mathcal{O}(\alpha_s^4) \quad , \tag{11}$$

where

$$
\begin{aligned}
w &= 1 - b_0 \alpha_s(\mu^2) \ln \frac{\mu^2}{q^2} \\
b_0 &= \frac{33 - 2n_f}{12\pi} \\
b_1 &= \frac{153 - 19n_f}{24\pi^2} \quad ,
\end{aligned}
\tag{12}
$$

with $n_f = 5$ being the number of active flavors. This second order solution is at the same time exact to all orders in leading and next-to-leading logarithmic accuracy.

The integral can be performed analytically. After dropping all terms of subleading order, the remaining part constitutes the leading and (incomplete) next-to-leading logarithmic prediction for y_3, including the scale dependence,

$$
\begin{aligned}
\frac{\pi b_0}{C_F} \ln R(y_3) &= - \left(1 + \frac{\ln(1-x)}{x} \right) \ln y_3 \\
&\quad + \frac{b_1}{b_0^2} \left(\frac{x + \ln(1-x)}{1-x} + \frac{1}{2} \ln^2(1-x) \right) - \frac{3}{2} \ln(1-x) \\
&\quad - \left(\frac{x}{1-x} + \ln(1-x) \right) \ln \frac{\mu^2}{s} \quad ,
\end{aligned}
\tag{13}
$$

with

$$x = -\alpha_s(\mu^2) \, b_0 \, \ln y_3 \quad . \tag{14}$$

References

[1] ALEPH collab., D. Decamp et al., *Phys. Lett* **B 255** (1991) 623.

[2] DELPHI collab., P. Abreu et al., *Phys. Lett.* **B 247** (1990) 167.

[3] L3 collab., B. Adeva et al., *Phys. Lett.* **B 248** (1990) 464;
L3 collab., B. Adeva et al., *Phys. Lett.* **B 271** (1991) 461.

[4] OPAL collab., M.Z. Akrawy et al., *Phys Lett.* **B 235** (1990) 389;
OPAL collab., M.Z. Akrawy et al., *Z. Phys.* **C 49** (1991) 375.

[5] MARK II collab., S. Komamiya et al., *Phys. Rev. Lett.* **64** (1990) 987.

[6] DELPHI collab., P. Abreu et al., *CERN preprint* **PPE/91-181** (1991).

[7] OPAL collab., P.D. Acton et al., *CERN preprint* **PPE/92-18** (1992).

[8] ALEPH collab., D. Decamp et al., *Phys. Lett.* **B 257** (1991) 479.

[9] DELPHI collab., P. Abreu et al., *Phys. Lett.* **B 252** (1990) 149.

[10] OPAL collab., M.Z. Akrawy et al., *Phys. Lett.* **B 252** (1990) 159;
OPAL collab., P.D. Acton et al., *CERN preprint,* **PPE/91-214** (1991).

[11] L3 collab., B. Adeva et al., *Phys. Lett.* **B 257** (1991) 469.

[12] R.K. Ellis, D.A. Ross and A.E. Terrano, Nucl. Phys. **B 178** (1981) 421.

[13] Z. Kunszt, P. Nason, G. Marchesini and B.R. Webber, *QCD,* in *Proceedings of the Workshop on Z Physics at LEP,* eds. G. Altarelli, R. Kleiss and C. Verzegnassi, CERN Report 89-08 (1989).

[14] S. Catani, G. Turnock, B.R. Webber and L. Trentadue, *Phys. Lett.* **B 263** (1991) 491.

[15] S. Catani, G. Turnock and B.R. Webber, *Phys. Lett.* **B 272** (1991) 368.

[16] S. Catani, Yu.L. Dokshitzer, M. Olsson, G. Turnock and B.R. Webber, *Phys. Lett.* **B 269** (1991) 432.

[17] ALEPH collab., D. Decamp et al., *Nucl. Instr. Meth.* **A 294** (1990) 121.

[18] ALEPH collab., *Properties of Hadronic Z Decays and Test of QCD Generators,* to be published.

[19] Durham Workshop, W.J. Stirling, *J. Phys.* **G**: *Nucl. Part. Phys.* **17** (1991) 1567;
N. Brown and W.J. Stirling, *RAL preprint* **91-049** (1991);
S. Bethke, Z. Kunszt, D.E. Soper and W.J. Stirling, *CERN preprint* **TH.6221/91** (1991).

[20] S. Catani, *CERN preprint* **TH.6281/91** (1991).

[21] P. Nason, program EVENT, private communication.

[22] G. Turnock, program NLLA, private communication.

[23] Yu.L. Dokshitzer and S. Troyan, *Leningrad preprint* **LNPI No. 922** (1984).

[24] G. Marchesini and B. Webber, *Nucl. Phys.* **B310** (1988) 461.

[25] T. Sjörstrand and M. Bengtsson, *Comp. Phys. Comm.* **43** (1987) 367;
M. Bengtsson and T. Sjörstrand, *Phys. Lett.* **B 185** (1987) 435, *Nucl. Phys.* **B 289** (1987) 810.

[26] B. Andersson, G. Gustafson, G. Ingelmann and T. Sjörstrand, *Phys. Rep.* **97** (1983) 31.

[27] S. Wolfram, in *Proc. 15th Rencontre de Moriond* (1980), ed. J. Tran Thanh Van;
G.C. Fox and S. Wolfram, *Nucl. Phys.* **B 168** (1980) 285.

[28] A.H. Mueller, *Phys. Lett.* **B 104** (1981) 161;
B.I. Ermolaev and V.S. Fadin, *JETP Lett.* **33** (1981) 269;
A. Bassetto, M. Ciafaloni, G. Marchesisni and A.H. Mueller, *Nucl. Phys.* **B207** (1982) 189;
Yu.L. Dokshitzer, V.A. Khoze, A.H. Mueller and S.I. Troyan, *Basics of Perturbative QCD*,
Editions Frontières, Paris (1991).

[29] I.G. Knowles, *Nucl. Phys.* **B 310** (1988) 571.

[30] J. Ellis, D.V. Nanopoulos and D.A. Ross *Phys. Lett.* **B 267** (1991) 132.

	Leading Log	Next-to-Leading Log	Subleading			
First Order	$\alpha_s L^2$	$\alpha_s L$	α_s	$\alpha_s \mathcal{O}\left(\frac{1}{L}\right)$		
Second Order	$\alpha_s^2 L^3$	$\alpha_s^2 L^2$	$\alpha_s^2 L$	α_s^2	$\alpha_s^2 \mathcal{O}\left(\frac{1}{L}\right)$	
Third Order	$\alpha_s^3 L^4$	$\alpha_s^3 L^3$	$\alpha_s^3 L^2$	$\alpha_s^3 L$	α_s^3	$\alpha_s^3 \mathcal{O}\left(\frac{1}{L}\right)$
Fourth Order	$\alpha_s^4 L^5$	$\alpha_s^4 L^4$	$\dots$	$\dots$	$\dots$	$\dots$
$\vdots$	$\vdots$	$\vdots$				

Table 1: Schematic representation of the order by order expansion of theoretical prediction in leading logarithms, next-to-leading logarithms and subleading logarithms.

	α_s from $-\ln y_3$ in range $[1.6, 4.0]$	α_s from $-\ln(1-T)$ in range $[1.2, 2.6]$	α_s from $-\ln(M_h^2/s)$ in range $[1.8, 2.8]$
Uncorrected value	0.1152	0.1314	0.1276
Corrected with:			
Lund PS	0.1221	0.1298	0.1231
HERWIG	0.1234	0.1246	0.1295
Lund-PS, no $\mathcal{O}(\alpha_s)$	0.1226	0.1272	0.1218
Average corrected value	0.1228	0.1272	0.1257

Table 2: Fit results for α_s from different hadronization corrections extrapolated to $Q_0 = 0$. The average corrected value is defined by the center of the range spanned by the different hadronization models. The theoretical predictions were applied with R matching and the scale parameter $f = 1$.
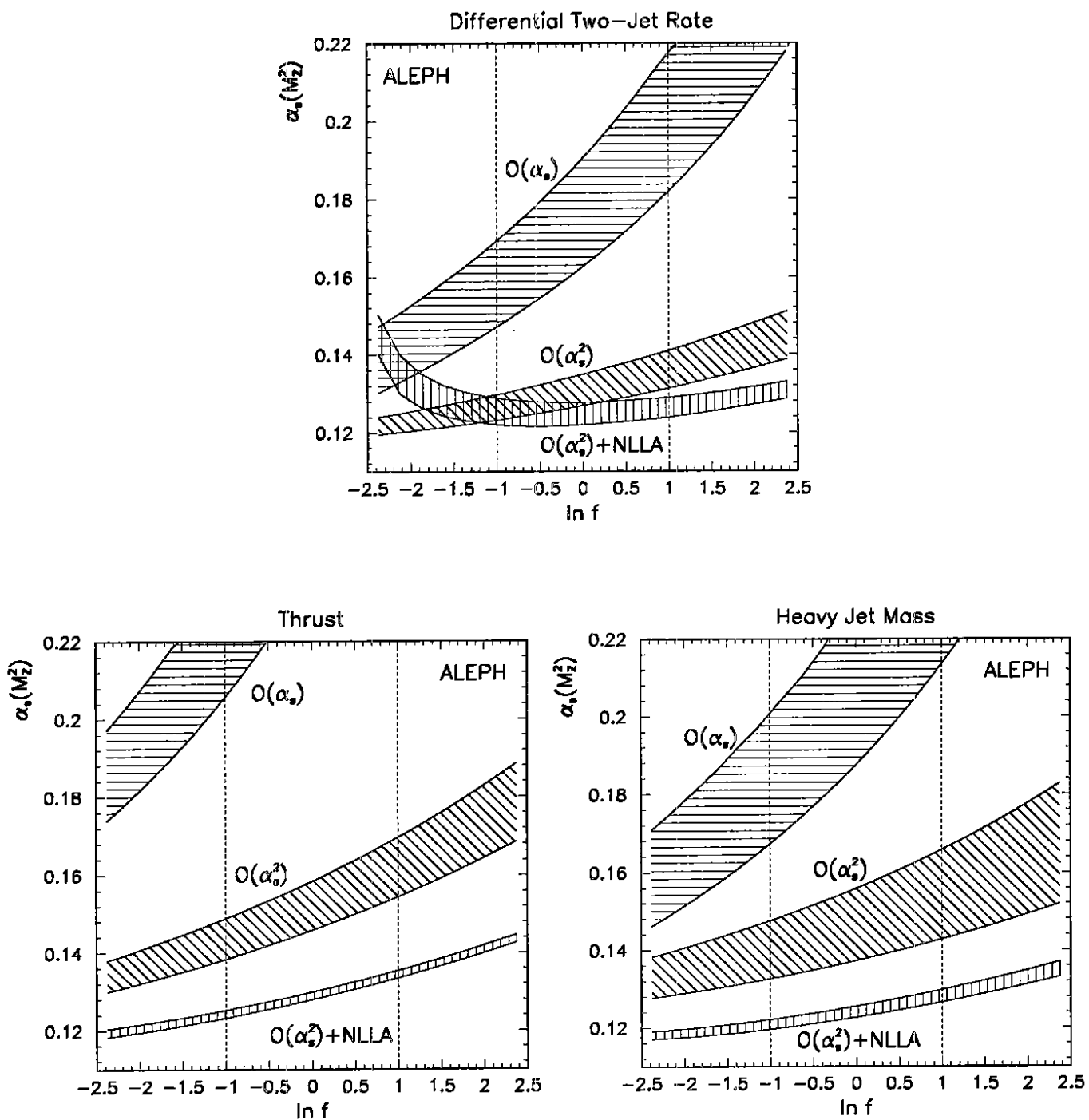
Figure 1: *Fit results for $\alpha_s(M_Z^2)$ as a function of the scale parameter for the variables y_3, T and ρ. The bands correspond to fits from first order, second order and complete predictions (see text). The width of the bands represents the matching dependence. The dotted vertical lines show the range in $\ln f$ used in the evaluation of the theoretical uncertainty.*
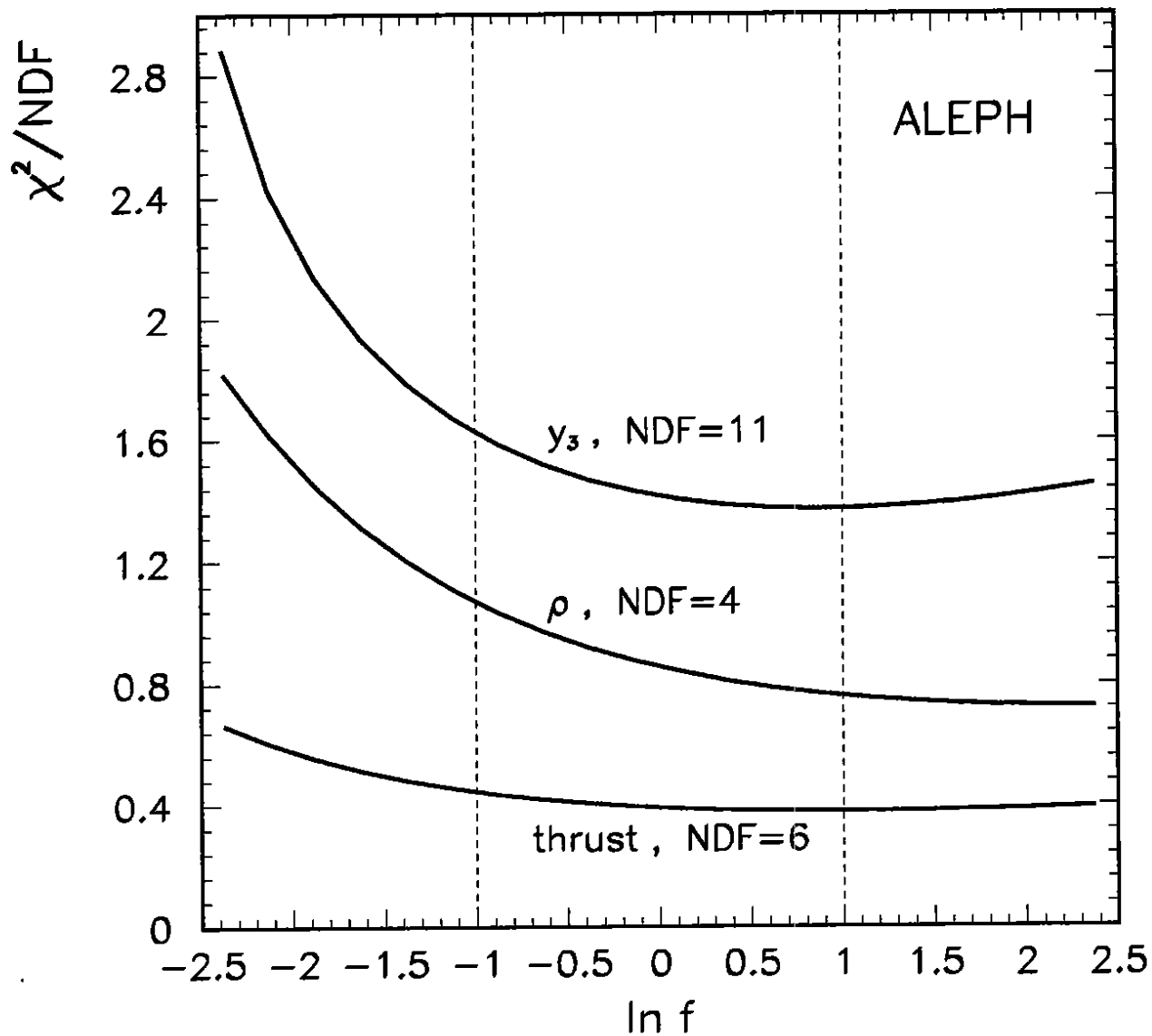
Figure 2: χ^2 per degree of freedom as a function of the scale parameter for the variables y_3, T and ρ. The R matching scheme was used and the hadronization corrections were taken from Lund PS. Only statistical errors in the data are taken into account in the fits.
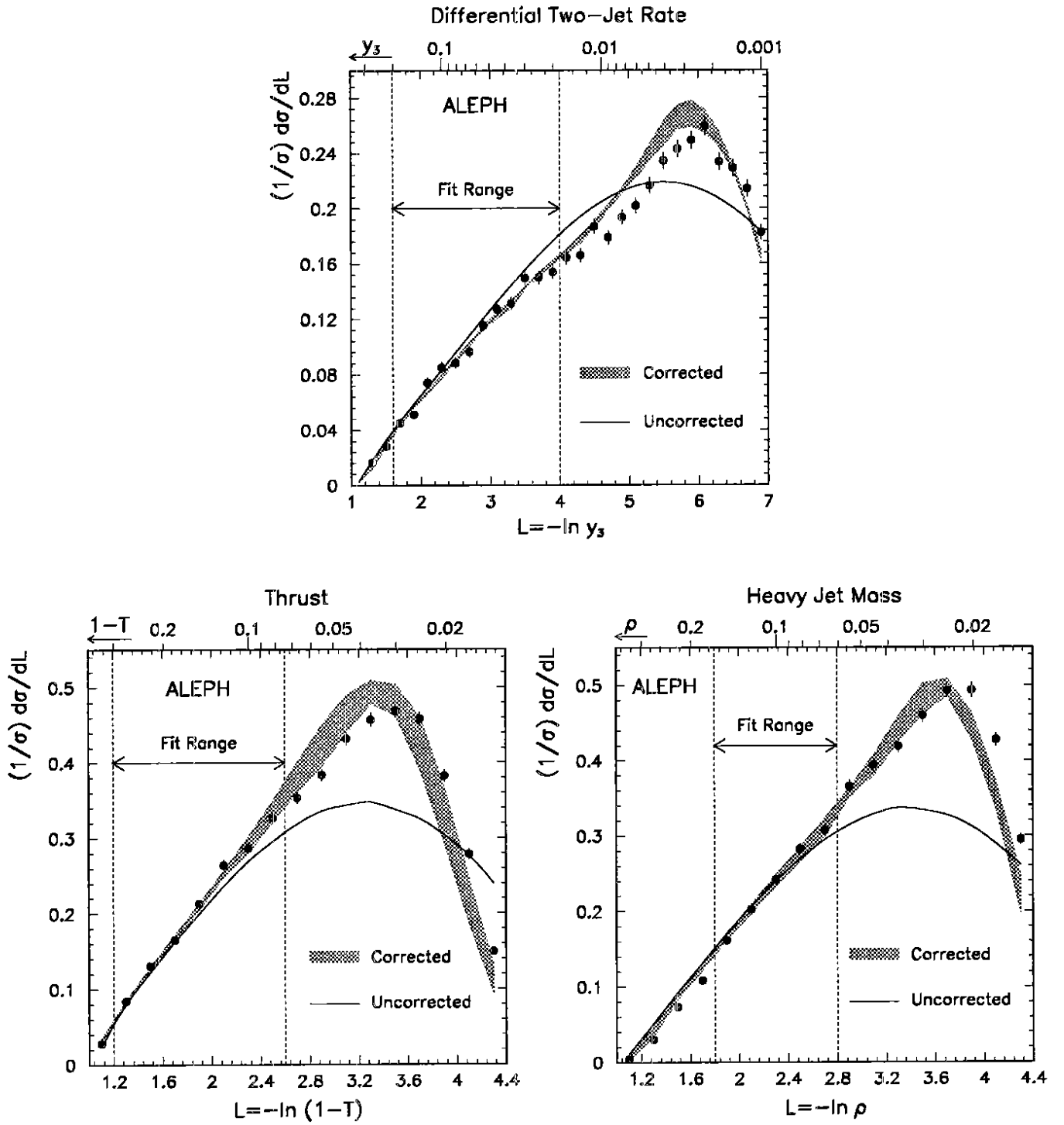
Differential Two—Jet Rate

Thrust

Heavy Jet Mass

Figure 3: *Experimental distributions (statistical errors only) together with bands covering the predictions using the three hadronization models and the central values of α_s for $f = 1$ and R matching. The curves are the predictions for the same values of α_s without hadronization corrections.*